DDES and OES Simulations of a Morphing Airbus A320 Wing and Flap in Different Scales at High Reynolds

Abderahmane Marouf, Nikolaos Simiriotis, J. B. Tô, Y. Bmegaptche, Yannick Hoarau, Marianna Braza

DDES and OES simulations of a morphing Airbus A320 wing and flap in different scales at high Reynolds.

A. MAROUF[1,2], N. SIMIRIOTIS[2], J.B. TÔ[2], Y. BMEGAPTCHE[2], Y. HOARAU[1], M. BRAZA[2]

[1] ICUBE, Unité Mixte C.N.R.S – Université de Strasbourg 7357, France
[2] Institut de Mécanique des Fluides de Toulouse (IMFT), UMR 5502 CNRS-INPT-UT3
Allée du prof. Camille Soula, 31400 Toulouse, France
amarouf@unistra.fr, nikolaos.simiriotis@imft.fr, jean-baptiste.to@imft.fr, yannick.bmegaptchetekap@imft.fr, hoarau@unistra.fr, marianna.braza@imft.fr

Abstract. The present study concerns the use of unsteady numerical simulations by means of Navier Stokes Multi Block (NSMB) solver including both high order schemes and turbulence resolving methods. Firstly, this work attempts to highlight the role of the morphing applied to the supercritical Airbus A320 wing and flap in the trailing-edge for a Reduced Scale (RS) prototype at the clean position, this morphing includes a slight deformation of the trailing edge with a selected frequency and amplitude, which has an impact on the flow near the trailing edge and specially in the wake structures. This solution can transform the 3-dimensional chaotic flow into a 2-dimensional one by enhancing coherence of 2D structures rows of von Kármán vortices. In Addition, the highlift A320 wing-flap at the take-off position in Large-Scale (LS) configuration have been studied using advanced hybrid models DDES, the Organised Eddy Simulation OES and SST for the RANS regions as well as LES Smagorinsky model.

Keywords: morphing, flap, wing, frequency, vibration, hybrid models

1 Introduction

Many studies in recent years have aimed at improving the aerodynamic performance of a wide range of aircraft (military, transport, commercial and general aircraft). As such, a large part of contribution in the literature is focused on the improvement of aerodynamic performance in the cruise, take-off and landing configurations by increasing lift and decreasing drag. The new family of airfoils, known as supercritical has demonstrated an improvement in the aerodynamic characteristics compared to the earlier airfoils. This study introduces a new technology based on wing and flap deformation using electroactive morphing in

the context of the H2020 Smart Morphing and Sensing a European project for Aeronautical Configurations www.smartwing.org/SMS/EU. Numerical simulations with hybrid turbulence models have been used in this study. Smart materials installed in the wing or the flap help to increase the aerodynamic performances and to decrease the aerodynamic noise in the wake. Several tests and simulations have been carried out to show the optimal vibration and the slight deformation of the trailing edge region. In the experimental set-up the actuation with a slight deformation is achieved through Micro-Fiber Composite (MFC) piezo-patches and the camber control is achieved by the Shape Memory Alloys (SMA) operating at low frequencies (order of 1 Hz), whereas the trailing-edge vibrations are of higher order (100-500 Hz). The combination of both actuations with the MFC and SMA, results in the hybrid morphing (G. Jodin *et al* 2017 [1]).

2 Numerical configuration and turbulence modeling

2.1 Flow configuration

The simulation of the A320 wing, concerns firstly the RS prototype (c=0.7 m) which was previously studied experimentally in our research group [1] [2]. This work was in the clean configuration and validated numerically by N. Simiriotis *et al* [3] by means of computations for a high angle of attack at 10° and a freestream Mach number of 0.06 which corresponds to a chord-based Reynolds number of approximately 1×10^6. In addition, deformable grid methods were used by means of a compressible Navier–Stokes code adopting the Organised Eddy Simulation model. Secondly the study illustrates the LS (c=2.72 m) with a two-element wing-flap in the take-off position of the A320 operating at a Mach number of 0.032 and chord-based Reynolds of 2.25×10^6. The attack angle is taken as 8° and compared to numerical and experimental results (W. LU *et al* [4]).

2.2 Numerical parameters

The NSMB code (Y. Hoarau [5]) is used to perform fluid dynamics simulation. The code solves unsteady and steady compressible Navier Stokes equations using the finite volume method, a structured grid is used to simulate the flow around single and two-element wing-flap. This includes a variety of efficient high-order numerical schemes and turbulence modelling closures in the context of URANS, LES and hybrid turbulence modelling. This code includes efficient fluid–structure coupling for moving and deformable structures. In the present study, the fourth-order central scheme and second order dual-time stepping for the temporal discretisation are selected. Preconditioning artificial compressibility was used to simulate the flow in a subsonic speed range for both reduced and large-scale configurations. A physical time step of 10 µs was validated for 3D simulation after a detailed investigation, a typical number 100 of inner iterations was mandatory for the process of convergence for each outer time step.

2.3 Boundary and initial conditions

No-slip conditions are employed on the wing wall and the presence of the wind tunnel walls are taken into account in the RS configuration. After several tests, the results obtained with a slip boundary condition for the upper and lower walls gave a better approximation to the experimental results than no-slip conditions and to avoid refinement near to the walls. On the other hand, far-field conditions are selected for the LS configuration with the characteristic variables extrapolated in time due to the complexity of the wind tunnel. Total pressure P0 and total temperature T0 are taken as standard conditions, as well as the upstream Reynolds numbers of 1×10^6 and 2.25×10^6 and Mach numbers of 0.062 and 0.032 respectively. The measurement of the upstream turbulence intensity in the wind tunnels of IMFT is 0.01 %. The initial solution is taken as a steady-state generated field in each case.

2.4 Turbulence modelling :

The following URANS and hybrid turbulence modelling models are chosen. Two-equation OES-k − ε [6] for the RS configuration, this model has the ability of the splitting the spectrum of energy based on organized coherent character. The coherent structures are resolved, and the random chaotic structures are modelled. In addition, hybrid DDES-k − ω SST and DDES-k − ε OES [8][9] models were used for the LS configuration. The activation of the ambient terms was necessary to prevent the free decay of the transported turbulence variables. The turbulent lenghscale l replaces the wall distance in the selected DDES models, this variable appears in the function f_d through the near-wall parameter and it is defined as :

$$l = d - f_d \max(0, d - C_{DES}\Delta_{max}) \quad (1)$$

Where C_{DES} is a constant and Δ_{max} is based on the largest dimension of the local grid cell.

The Figure.1 represents the f_d and the non-dimensional streamwise velocity near wall regions, 6 positions are selected (near to leading edge, medium and trailing edge) of the upper surfaces in the wing and the flap. The switch from RANS to LES in all the cases is rapid and the f_d slope in the switching area is close to 0 (horizontal line). The flow is separated at the end of the wing (*x/c=0.59*) and the flap (*x/c=0.9*, *x/c=0.98*) and the thickness of the RANS layers are almost the same 10^{-3} to 1.5. $10^{-3}\ z/C$, but the switch to LES happens inside the boundary layer compared to the other positions where no separation occurs. The delaying function f_d tends to 0 in the RANS regions and 1 in LES regions (where $r_d << 1$)

$$f_d = 1 - \tanh[(8r_d)^3] \qquad r_d = \frac{\nu_t + \nu}{S_d k^2 d^2} \qquad S_d = \sqrt{\frac{\partial u_i}{\partial x_j} \cdot \frac{\partial u_i}{\partial x_j}} \tag{2}$$

As can be seen in Eq. (2), the turbulence length scale in DDES is also function of the local state of the flow by means of the eddy viscosity and the deformation tensor.

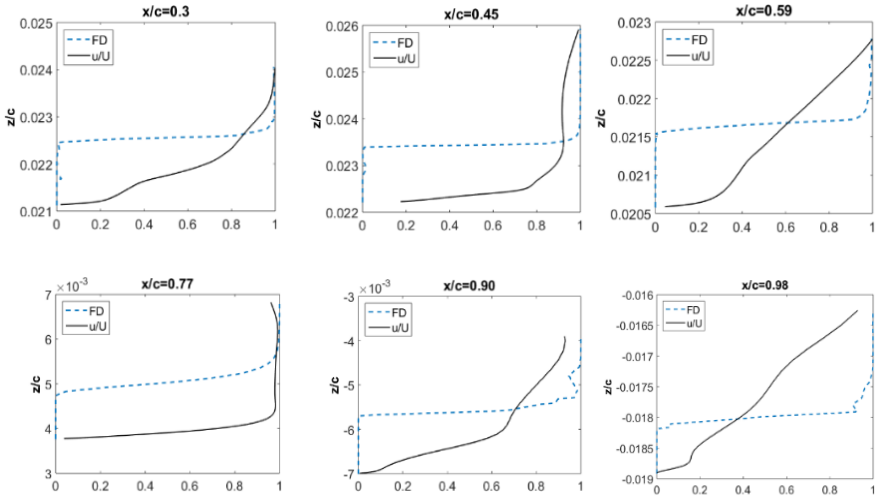

Fig. 1. Presentation of the DDES-k − ω SST delaying function FD and the non-dimensional streamwise velocity in six chosen positions over the wing and the flap.

2.5 Grid generation and deformation

Multiblock structured grids were generated to simulate the flow around the RS and LS configurations as presented in the Figure. 2. The RS grid contains 20 million cells with a minimum local cell size less than 1 mm is defined near to the trailing-edge of the wing to capture the flow detachment. A spanwise of 0.8C (80 cells in the span direction), which is sufficient for the OES model, the mesh was created similar to the IMFT wind tunnel with 11C for the total domain from the inlet to the outlet and the wing is placed in the middle. In the other hand, the LS grid has 30 million cells with a spanwise of 0.11C (40 cells in the span direction), in addition a far-field boundary conditions were selected with 20C. The Arbitrary Lagrangian Eulerian (ALE) [9] is used in order to solve dynamic problems involving large and small deformations. This method is applied for the trailing edge of the wing in the RS configuration and in the flap for the LS configuration, the deformation is imposed each time step following a sinusoidal movement highlighted in the Figure. 3. The inner iterations help the convergence of the solution and this needs to be readapted for high frequency deformation to achieve a high accuracy.

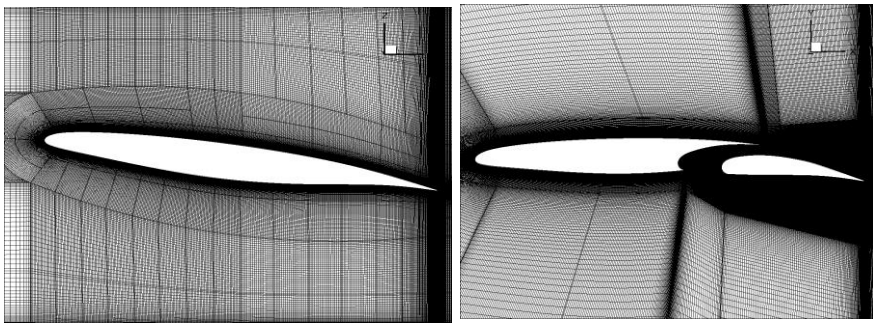

Fig. 2. Slice of the different grids. (left) **:** Reduced Scale at the clean position. (right) : Large Scale at the take-off position.

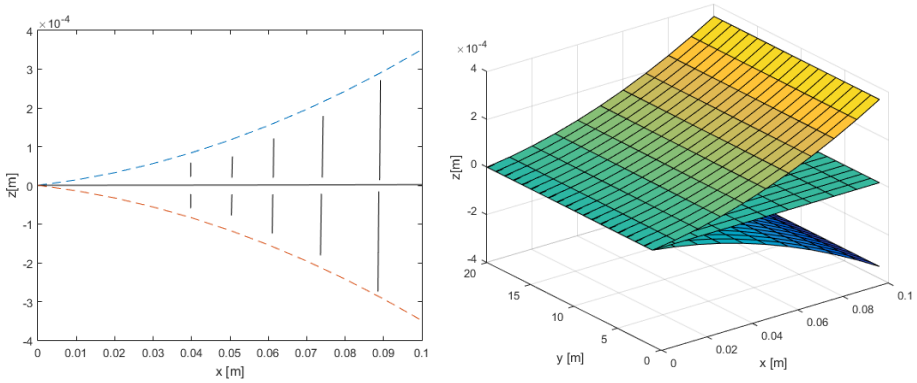

Fig. 3. Presentation of the trailing-edge movement using the ALE method.

The vibration of the trailing-edge is controlled by means of the actuation frequency, the amplitude and the *x* displacement. These parameters are defined by the user as input to calculate the real displacement of each cell in every time step and compute the grid deformation. In the RS prototype the wing's trailing-edge is selected in the morphing configuration and in the LS prototype the flap's trailing-edge will be morphed. An imposed small deformation of 0.35mm and high frequency of 300 Hz were selected as optimal configuration for the dynamic morphing based on our previous studies.

3 Results and discussion

3.1 RS configuration

This part of the study focuses on the RS in clean configuration (c=0.7 m). Using the k-ε-OES, the resolved turbulence corresponds to an ensemble averaged flow evolution, representing the organized, coherent part of the flow. The homogeneous ambient terms are activated and described in Spalart and Rumsey (2007) [9]. In addition, the $C_{mu}=0.03$ has shown an improvement in the boundary layer separation near the trailing edge compared to the Standard k-ε model $C_{mu}=0.09$.

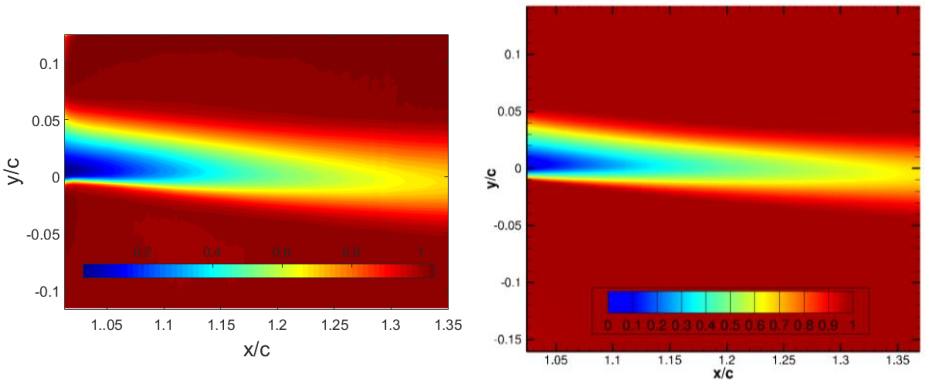

Fig. 4. Comparison of experimental and numerical results. (left) : PIV results from IMFT by G. Jodin. (right) : 3D numerical results

A preconditioning method was tested based on the artificial compressibility in our compressible solver NSMB in the implicit dual time stepping method Lower Upper Symmetric Gauss Seidel (LU-SGS). This preconditioning gave approximate results to experimental data but a thinner wake deficit as presented in the Figure. 4. This is caused by the presence of the wind tunnel walls in the upper, lower and sided parts of the wing prototype, which were taken as slip conditions in numerical simulations. Another reason is the confinement of the wind tunnel, we think that the Reynolds number is slightly higher in the experimental than the numerical simulation.

Figure. 5 presents a first overview of the morphing *(with vibration)* by means of the ALE grid deformation in the 3D RS configuration compared with the static *(no vibration)* showing the iso-surfaces of the Q criterion at a fixed value of 1500 and colored by the vorticity magnitude. This highlights the morphing effects in the spanwise direction and the wake behavior.

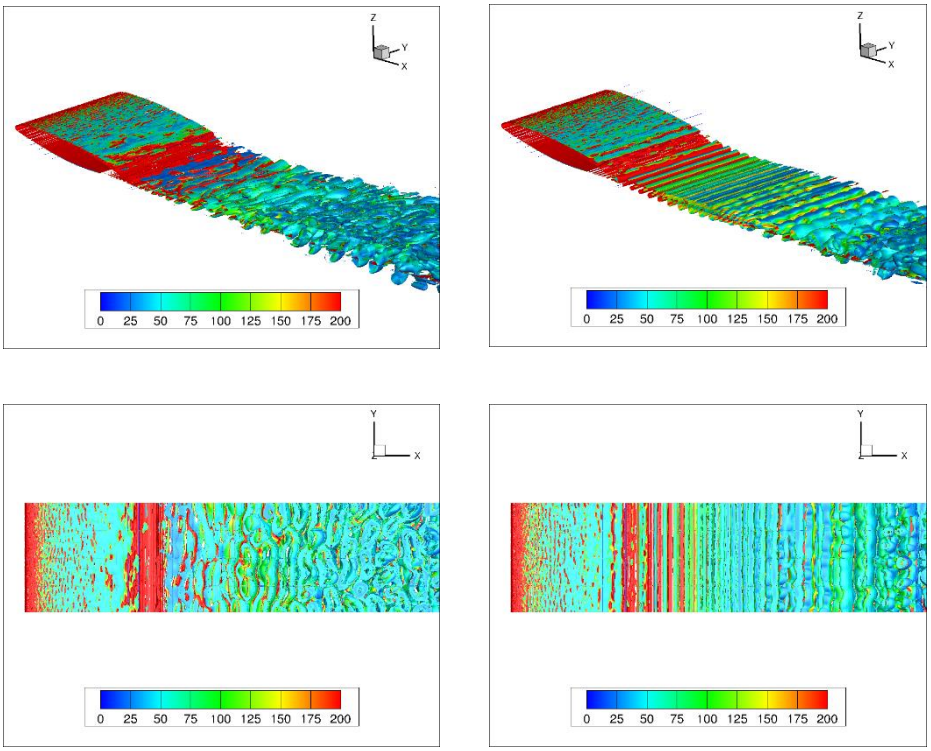

Fig. 5. : Visualization of the iso-surfaces of Q criterion = 1000 colored by the velocity magnitude around the wing in clean configuration. Left : morphing case at 300 Hz *(with vibration)* and (right) : static case *(no vibration)*.

The suppression of the 3-dimensional instabilities in the spanwise direction is illustrated in the Figure. 5. The undulation that occurs as an inherent characteristic of the flow in the static case is obtained by the Organized Eddy Simulation model due to the non-linear interaction of turbulent structures at high Reynolds number. The evolution of the velocity magnitude appears clearly in the spanwise in Figure. 5 and displays an undulation with an irregular wavelength (chaotic flow) of von Kármán rows. Longitudinal vorticity ω_x is clearly present in the spanwise direction for the static case. However, added to the wake flow some energy introduced by the vibration at the frequency 300 Hz and a slight deformation in the trailing edge, can suppress the three-dimensional undulation and transforms the wake flow into quasi two-dimensional. This helps to increase the lift with some percentage and decrease the pressure drag which is associated with the turbulence structures created in the

wake flow at high Reynolds and angle of attack. Several simulations for a specific range of frequency and deformation have been tested to find the most appropriate configuration to show the good effects of the morphing wing.

3.2 LS configuration

This part of the study concerns the highlift two-element airfoil at a large scale (c=2.72 m). The design of the DDES grid around the airfoil-flap requires a homogenous local grid cells with $\Delta_x \approx \Delta_y \approx \Delta_z$ following the recommendations of Spalart in the LES region. Two different hybrid models SST-DDES and OES-DDES have been chosen to simulate the flow around the LS wing-flap configuration Figure**.** 7. The classical Smagorinsky model for LES has been selected and the DES subgrid length-scale is taken as $\Delta_{max}=max(\Delta_x, \Delta_y, \Delta_z)$.

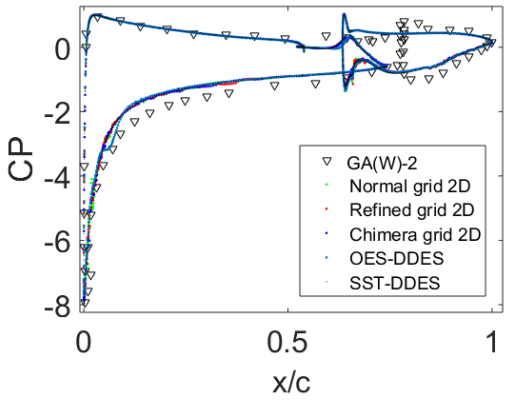

Fig. 6. Pressure coefficient of the wing-flap LS configuration for different grid

Time step validation was carried out for 2D grids. Several tests with different values of $\Delta t = 10^{-3}, 10^{-4}$ and 10^{-5} seconds were tested to find out the optimal time step. A 10^{-5} seconds was sufficient and was adopted for the simulations. A typical number between 60 and 100 inner steps was sufficient for the convergence in each time step. The grid independency is presented in Figure. 6. Comparing 2D normal, refined, Overset (Chimera) grids and the 3D grid tested with OES-DDES and SST-DDES, almost the same accuracy was shown with 2D results. Another comparison with W. Lu *et al* [3] results of GA (w) 2 wing-flap and the A320 at the same flow configuration and speed in Figure. 6 was tested. Numerical simulations show a good approximation to GA (w) 2 in CP distribution around the wing, but there is a small change in the upper surface of the wing due to the difference of shape. Notice that in GA (w) 2 flap is smaller than the A320 which explains the reason of the difference in the pressure distribution. Even though we still have a good agreement between both configurations.

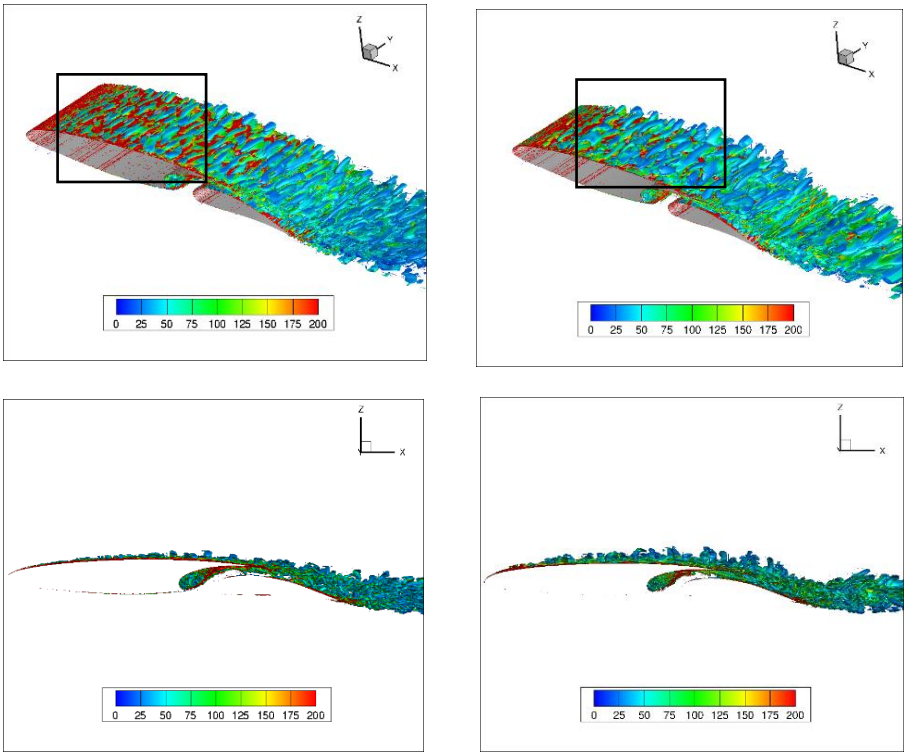

Fig. 7. Presentation of the Q criterion = 1000, colored by the velocity magnitude, (left) : DDES-k − ω SST and (right) DDES-k − ε OES. 3 dimensional in the (x,y,z) on the top and a plane (x,z) taken from the middle down.

To illustrate the flow regions, Figure. 7 provides a view of the turbulence structures visualized by the iso-surfaces of the Q criterion colored by the velocity magnitude above the wing and in the wake by means of the SST-DDES and OES-DDES. The SST shows less solved turbulent structures compared to the OES which generates relatively large structures. This is caused by the modification of the constant C_{mu} for the OES model in the URANS region to predict the behaviour of the boundary layer detachment before switching to the LES Smagorinsky model better than the standard URANS models.

4 Conclusion

High fidelity OES and hybrid RANS/LES models contributed to these relevant challenging test cases, providing results of single element in the clean RS configuration and two-element wing-flap in take-off LS configuration. In addition, an imposed deformation *(with vibration)* on the trailing edge to the single element

RS wing using OES model in the clean RS configuration results in a completed elimination of the 3D effects in the spanwise direction of the wake, this can make the wake thinner. A decrease of the drag and an increase of the lift of some percentage have been noticed for low and high frequencies actuations in the morphing configuration. Thus, showing that the OES model does not require a refined mesh as hybrid models to capture 3 dimensional effects in the wake. In addition, the second part of the study hybrid models have been used and tested, the OES-DDES showed a better resolution of the turbulent structures compared to SST-DDES.

In perspectives of this study, the morphing *(with vibration)* cases under hybrid simulations as DDES for single and two element wing-flap in the future will be tested and this will probably illustrate more what will be modified in the smaller scales that are resolved in the wake.

References

1. G. Jodin, V. Motta, J. Scheller, E. Duhayon, C. Doll, J.F. Rouchon, M. Braza. : Dynamics of hybrid morphing wing with active open loop vibrating trailing edge by time-resolved PIV and force measures. Journal of Fluids and Structures, 74, pp. 263-290 (2017)
2. J. Scheller, M. Chinaud, JF. Rouchon, E. Duhayon, S. Cazin, M. Marchal, M. Braza : Trailing-edge dynamics of a morphing NACA0012 aileron at high Reynolds number by high-speed PIV. Journal of Fluids and Structures 55 (2015) 42–51
3. N. Simiriotis, G. Jodin, A. Marouf, Y. Hoarau, J.F. Rouchon and M. Braza : Electroactive morphing on a supercritical wing targeting improved aero-dynamic performance and flow control in high Reynolds numbers. 53rd 3AF International Conference on Applied Aerodynamics 26 – 28 March 2018
4. Weishuang LU, Yun TIAN, Peiqing LIU : Aerodynamic optimization and mechanism design of flexible variable camber trailing-edge flap. Chinese Journal of Aeronautics. (2017), 30(3): 988–1003.
5. Y. Hoarau, D. Pena, J. B. Vos, D. Charbonier, A. Gehri, M. Braza, T. Deloze, and E. Lau- rendeau : Recent Developments of the Navier Stokes Multi Block (NSMB) CFD solver. In 54th AIAA Aerospace Sciences Meeting. American In- stitute of Aeronautics and Astronautics.
6. R. Bourguet, M. Braza, G. Harran, and R. El Akoury : Anisotropic Organised Eddy Simulation for the prediction of non-equilibrium turbulent flows around bodies. Journal of Fluids and Structures, 24(8):1240–1251, November 2008
7. P. R. Spalart, C. L. Rumsey : Effective Inflow Conditions for Turbulence Models in Aerodynamic Calculations. AIAA Journal, Vol. 45, No. 10 (2007), pp. 2544-2553.
8. P. R. Spalart, : Detached-Eddy Simulation,"Annual Review of Fluid Mechanics, Vol. 41, No. 1, 2009, pp. 181–202. URLhttps://doi.org/10.1146/annurev.fluid.010908.165130.
9. J. Donea, S. Giuliani, and J. P. Halleux : An arbitrary lagrangian-eulerian finite element method for transient dynamic fluid-structure interactions. Computer Methods in Applied Mechanics and Engineer- ing, 33(1):689–723, September 1982